Journal of Nuclear Materials 508 (2018) 472–480

Contents lists available at ScienceDirect

Journal of Nuclear Materials

journal homepage: www.elsevier.com/locate/jnucmat

Expanding the capability of reaction-diffusion codes using pseudo traps and temperature partitioning: Applied to hydrogen uptake and release from tungsten

M.J. Simmonds [a, *], J.H. Yu [a], Y.Q. Wang [b], M.J. Baldwin [a], R.P. Doerner [a], G.R. Tynan [a, c]

[a] Center for Energy Research, UC San Diego, 9500 Gilman Dr., La Jolla, CA, 92093-0417, USA
[b] Materials Science and Technology Division, Los Alamos National Laboratory, Los Alamos, NM, 87545, USA
[c] Department of Mechanical and Aerospace Engineering (MAE), UC San Diego, 9500 Gilman Dr., La Jolla, CA, 92093-0411, USA

ARTICLE INFO

Article history:
Received 28 October 2017
Received in revised form
21 May 2018
Accepted 31 May 2018
Available online 4 June 2018

Keywords:
Tungsten
Deuterium
Retention
TMAP
Ion beam damage
NRA
TDS

ABSTRACT

Simulating the implantation and thermal desorption evolution in a reaction-diffusion model requires solving a set of coupled differential equations that describe the trapping and release of atomic species in Plasma Facing Materials (PFMs). These fundamental equations are well outlined by the Tritium Migration Analysis Program (TMAP) which can model systems with no more than three active traps per atomic species. To overcome this limitation, we have developed a Pseudo Trap and Temperature Partition (PTTP) scheme allowing us to lump multiple inactive traps into one pseudo trap, simplifying the system of equations to be solved. For all temperatures, we show the trapping of atoms from solute is exactly accounted for when using a pseudo trap. However, a single effective pseudo trap energy can not well replicate the release from multiple traps, each with its own detrapping energy. However, atoms held in a high energy trap will remain trapped at relatively low temperatures, and thus there is a temperature range in which release from high energy traps is effectively inactive. By partitioning the temperature range into segments, a pseudo trap can be defined for each segment to account for multiple high energy traps that are actively trapping but are effectively not releasing atoms. With increasing temperature, as in controlled thermal desorption, the lowest energy trap is nearly emptied and can be removed from the set of coupled equations, while the next higher energy trap becomes an actively releasing trap. Each segment is thus calculated sequentially, with the last time step of a given segment solution being used as an initial input for the next segment as only the pseudo and actively releasing traps are modeled. This PTTP scheme is then applied to experimental thermal desorption data for tungsten (W) samples damaged with heavy ions, which display six distinct release peaks during thermal desorption. Without modifying the TMAP7 source code the PTTP scheme is shown to successfully model the D retention in all six traps. We demonstrate the full reconstruction from the plasma implantation phase through the controlled thermal desorption phase with detrapping energies near 0.9, 1.1, 1.4, 1.7, 1.9 and 2.1 eV for a W sample damaged at room temperature.

1. Introduction

The modeling of tritium fuel trapping and retention within neutron damaged W is of primary concern to next step fusion devices. In addition to the degradation of material properties, the accumulation of tritium has safety requirements regulated by the Nuclear Regulatory Commission [1]. Aside from transmutation and radioactivity, many of the fundamental aspects of neutron damage and tritium retention can safely be studied with the use of heavy ions and deuterium (D), respectively.

The primary experimental techniques for studying hydrogenic retention in W are Nuclear Reaction Analysis (NRA) and Thermal Desorption Spectroscopy (TDS). NRA utilizes a ^{3}He ion beam to probe the D concentration up to several microns in depth. This technique does not differentiate as to which type of trap holds the D, nor if it is in solution between lattice sites, but can infer the spatial distribution of D contained within the damaged materials.

* Corresponding author.
E-mail address: msimmonds@eng.ucsd.edu (M.J. Simmonds).

https://doi.org/10.1016/j.jnucmat.2018.05.080
0022-3115/

With TDS, the sample temperature is linearly increased and the surface flux of desorbed D is measured as a function of temperature. The flux of D from the sample is complicated by the multi-step migration process of diffusion, trapping, release, and eventual surface recombination to escape the sample. By modeling these coupled processes, TDS can reveal the energy required to escape a given trap. The release behaves as an Arrhenius process, in that an atom is trapped within an energy barrier and may escape once the atom acquires enough kinetic energy via random collisions.

Previous experiments studying the release of D from W through TDS have observed a range of release peaks at different temperatures, leading to a variety of inferred detrapping energies ranging from 0.65 to 2.4 eV [2–7]. Release peaks may shift in temperature due to various experimental effects. In the case of heavy ion damaged samples, the most significant factor that affects the release peaks is the damage depth profile. Samples with D filling traps formed by damage cascades deeper within the material will have further to migrate before reaching the surface, and thus have a higher probability of retrapping prior to reaching the surface, which leads to a broadening of the release peak and a shift towards higher temperature. Analysis of the release peaks is further obfuscated by the overlapping and coupling of traps due to a range of detrapping energies. In addition, traps with low detrapping energies may be missed entirely when sample temperature during the atomic implantation phase approaches or exceeds its low temperature release peak, preventing that trap from being populated and subsequently inferred through NRA or TDS measurements.

Though no ion source will produce the same damage as 14 MeV fusion neutrons 8, many of the resultant defects' fundamental properties can be explored. We do note that experiments utilizing ion damage may have experimental data that in turn produces more reliable inferred detrapping energies. Samples with uniform trap concentrations, such as undamaged or neutron damaged samples, may never saturate the filled trap concentration causing atoms escaping low energy traps to diffuse and further populate high energy traps deeper into the material. This can result in the filling of traps that are located beyond 10 μm depth. The subsequent TDS of such traps results in significant broadening of the release peaks, causing adjacent peaks to overlap and further obscuring the inferred detrapping energies. Unlike an undamaged or neutron damaged sample, the damage profile from heavy ions has a distinct depth and shape localized to the near surface region that can be modeled with the Stopping Range of Ions in Material (SRIM) [9]. Using this ion-induced damage spatial profile as a constraint, the resultant release peaks seen in experimental TDS data have a specific origin, increasing the confidence in the inferred detrapping energies. Note that the dpa profile predicted by SRIM does not take temperature into account [10]. The annealing of defects during or post damage will alter the shape of the profiles for surviving defects.

In order to infer the detrapping energies from TDS release peaks, a reaction-diffusion model must be used to simulate the experimental conditions. The Tritium Migration Analysis Program (TMAP) is a well validated and verified code used extensively within both the fission and fusion communities to simulate hydrogenic retention measurements [11–13]. The current version of TMAP7 can model up to three coupled traps simultaneously and was used to model the D implantation and thermal desorption phases of a recent experiment [14]. In our present work, we find that three traps cannot reasonably model the experimental data. To model a larger number of traps concurrently within the TMAP7 framework, we introduce a new PTTP scheme and show that it can effectively model the trapping and release of D from damaged W that exhibits trapping and release in six distinct traps.

2. TMAP7 simulation

As described in detail in Ref. [14], W samples were simultaneously damaged and annealed prior to D implantation in the PISCES-E RF plasma device. The simulation of D retention in W can be separated into three phases: the sample preparation, D implantation, and thermal desorption of D. Phase 0, sample preparation, produces the initial concentration of various defects that act as traps. Phase I, D implantation, entails the diffusion of D within the W lattice and the gradual filling of traps encountered by the diffusion front. Phase II, thermal desorption, is defined by the release of D from filled traps by controlled heating of the W sample. Table 1 below provides a summary of the relevant experimental parameters utilized in this simulation. In what follows, the sample damaged at room temperature is modeled.

Simulating the implantation phase, values for mean implantation depth (~4 nm) and surface ion reflection coefficient (~0.65) were taken from Eckstein [15]. To achieve consistency between modeled depth profile, thermal desorption, and experiment, either recombination, reflection, or re-emission must be increased for high incident ion flux during the implantation phase. The peak solute D concentration in the implantation zone is limited by one of these processes. This peak concentration also determines the D gradient that in turn drives the overall D diffusing into the bulk where it can be retained. Here the recombination coefficient could be taken as instantaneous to shift the release rate limiting process from surface release to diffusion. Instead, in order to retain the physics of recombination during the thermal desorption phase, we chose to increase the surface ion reflection coefficient (R) above the quoted Eckstein value. The incident ion flux ratio, Γ_{in}/Γ_{ion}, that penetrates the surface and is then implanted, was taken to be 8×10^{-4}, where $\Gamma_{in}/\Gamma_{ion} = 1 - R$. This degree of reduction is consistent with what was required to match results in other relatively high ion flux experiments [16]. Note that a similar implantation profile can be achieved using Eckstein's reflection coefficient when recombination is neglected and instantaneous surface release is modeled. The mechanism that reduces the D retained during implantation needs further experimental investigation. This is currently an unresolved issue that highlights the difficulty in the application of reaction diffusion physics to the uptake of hydrogenic isotopes in tungsten.

The D filled trap sites shown in the NRA experimental data (thick black) in Fig. 1 occupy three different spatial zones: the near surface implantation zone (~70 nm), the heavy ion damage zone (~1 μm), and the intrinsic defects throughout the rest of the sample. The W samples were initially annealed below the recrystallization temperature, which leaves behind a presumably uniform distribution of residual intrinsic defects. A uniform concentration of intrinsic traps was therefore assumed throughout the 1.5 mm thick sample. The spatial profile of D detected by NRA largely coincides with the spatial location of heavy ion damage predicted by SRIM [8]. As a result, in this work the concentration of Cu ion induced defects shown in Fig. 1 is assumed to have the SRIM spatial profile (red). Within 70 nm of the surface region, the NRA measurements of D retention shows defects were created and populated by D implantation, possibly due to lattice stresses induced by the incident plasma ion flux [6,17]. Shown on the log-log plot, the implantation zone is a small contribution to the total D retention and, therefore, simply modeled as a step function up to 70 nm. Since NRA measures the sum of all D filled traps, the detrapping energy of each trap cannot be determined without simulating the thermal desorption phase. As such, the concentration of each trap within each of these three zones is a free parameter, constrained by both the sum of filled traps after implantation (i.e. the spatial D profile from NRA) and the surface flux profile from TDS.

Table 1
Summary of detailed experimental conditions used as inputs to the TMAP7 modeling.

Phase 0 (Sample Preparation)
1.5 mm thick polycrystalline W
Annealed at 1173 K
3.4 MeV Cu ion damage
SRIM disp. damage threshold of 90 eV
0.2 peak dpa (Kinchin-Pease)
Simultaneous heating during damage
Temperatures spanning 300–1243 K
Phase I (D Implantation)
D2 plasma exposure for 50 min
Flux average of 3.3×10^{20} D/m^2
Fluence of 10^{24} D/m^2
Ion energy 110 eV
Sample temperature 383 K
20 min to cool down to RT
NRA - D concentration up to 6 μm
Phase II (Thermal Desorption)
Linear temperature ramp 0.5 K/s
Peak temperature of 1273 K

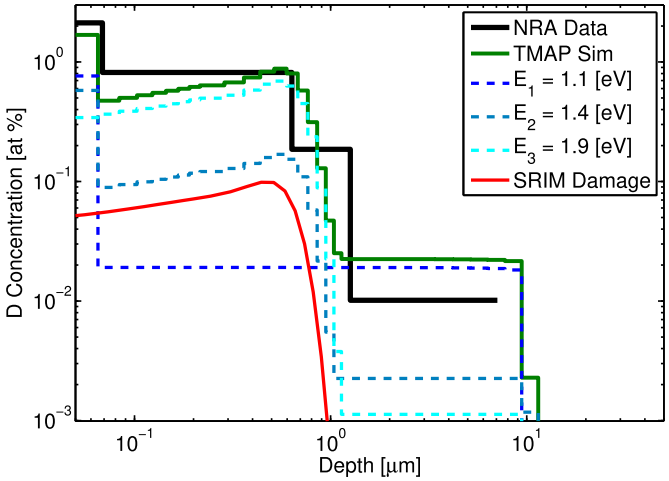

Fig. 1. Traps 1–3 (dashed lines) are simulated using TMAP and the sum total (green) is compared to experimental NRA data (thick black) with a NRMSE of 0.7. Note that the heavy ion damage profile simulated in SRIM (red) defines the spatial profile of induced traps used in TMAP shown with arbitrary units on the y-axis. (For interpretation of the references to colour in this figure legend, the reader is referred to the Web version of this article.)

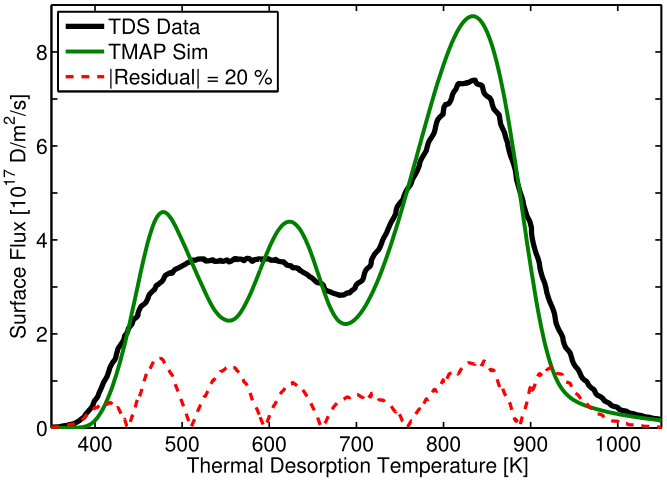

Fig. 2. The residual error (dashed red) shows the difference between the TMAP simulated release peaks (green) and the experimental TDS data (thick black) with a NRMSE of 0.7. (For interpretation of the references to colour in this figure legend, the reader is referred to the Web version of this article.)

In order to illustrate the need for the new approach proposed here, we model the experiment utilizing TMAP7 with three detrapping energies using an input file that was prepared with the parameters outlined above. Relevant constants such as Anderls recombination coefficient and the mass corrected Fraunfelder diffusion constant are well outlined by Poon et al. [7]. Phase I and II are simulated in order to establish a self-consistent solution to the NRA and TDS experimental data. The resultant concentrations of traps due to intrinsic defects and heavy ion damage present after Phase 0 are assumed constant. The plasma exposure modeled in Phase I produces further defects in the implantation zone. Due to the high ion flux and rapid surface saturation, the defects induced during Phase I likely formed in the first few seconds, relatively short compared to the total exposure of nearly an hour. Therefore the near surface implantation induced trap concentration is also assumed to be constant and an initial condition prior to the start of Phase I.

In Figs. 1 and 2, the best-fit NRA profiles and TDS release history from the TMAP7 simulation are shown for a W sample damaged at RT. Here the best-fit is determined by an iterative process of adjusting the various free parameters (e.g. trap concentrations) and comparing the resultant simulation against the experimental NRA and TDS measurements. The experimental and simulation data were interpolated on a finely spaced linear grid in order to determine the "Goodness of Fit." The Normalized Root Mean Square Error (NRMSE) was chosen as the figure of merit, where 1 would be a perfect fit of simulation to experimental data. Relative to the uncertainty in experimental NRA data, the three-trap TMAP fit to the NRA trapped D profile is acceptable. However, the thermal desorption profile obtained from the same sample, seen in Fig. 2, has a significant residual error that measures the unaccounted trapping and suggests the presence of more than three detrapping energies.

In recent work [14], we showed that three release peaks were clearly observable in the TDS data and well fit by three Gaussians. Initially, the area under each Gaussian was used to constrain the D inventory for each trap. Subsequently, the experimental conditions

were simulated with TMAP7 as described above; however, the calculated TDS profile could not accurately replicate both the experimental NRA and TDS data as seen in Fig. 2. In retrospect, the Gaussians were found to be unphysical in that their width were not the result of only three traps. Relaxing the total area constraint and thereby allowing the traps to vary in concentration does not yield a better fit. Only when using unphysical values, by significantly decreasing the diffusion coefficient or ignoring the NRA profile to increase the depth of trapped D could we broaden the release peaks to match the experimental TDS data.

Further examination of the TDS data suggests the existence of additional traps. In particular, although not easily seen in the total D flux, the D2 and especially the HD flux reveal additional release peaks as shown in Fig. 3. These results suggest the presence of six release peaks with distinct detrapping energies. Here we note that the lowest release peak in the present TDS data is not well resolved and may occur at a slightly lower temperature since it is only partially filled and obscured by the next nearest peak at 500 K. As mentioned previously, the values used to model the detrapping energies associated with these release peaks range from 0.65 to 2.4 eV [2–7]. The lowest and least resolved peak has an energy below the ~1.1 eV associated with the 500 K peak. These two peaks are clearly the dominant traps present in undamaged W. The four higher temperature release peaks are due to the heavy ion induced damage. Assuming that the spatial distribution for these four traps follows the damage profile computed with SRIM as shown in Fig. 1, and using the previously quoted values, the rest of the detrapping energies appear to be near 1.4, 1.7, 1.9, and 2.1 eV. While these detrapping energies are initially a free parameter, they are constrained by the complete experimental data set for all the TDS profiles annealed at various temperatures seen in Fig. 3. Motivated by the desire to model the D release from all six traps seen here in a manner that is consistent with NRA profiles and physically plausible diffusion rates for D in solution, we developed the PTTP scheme described below.

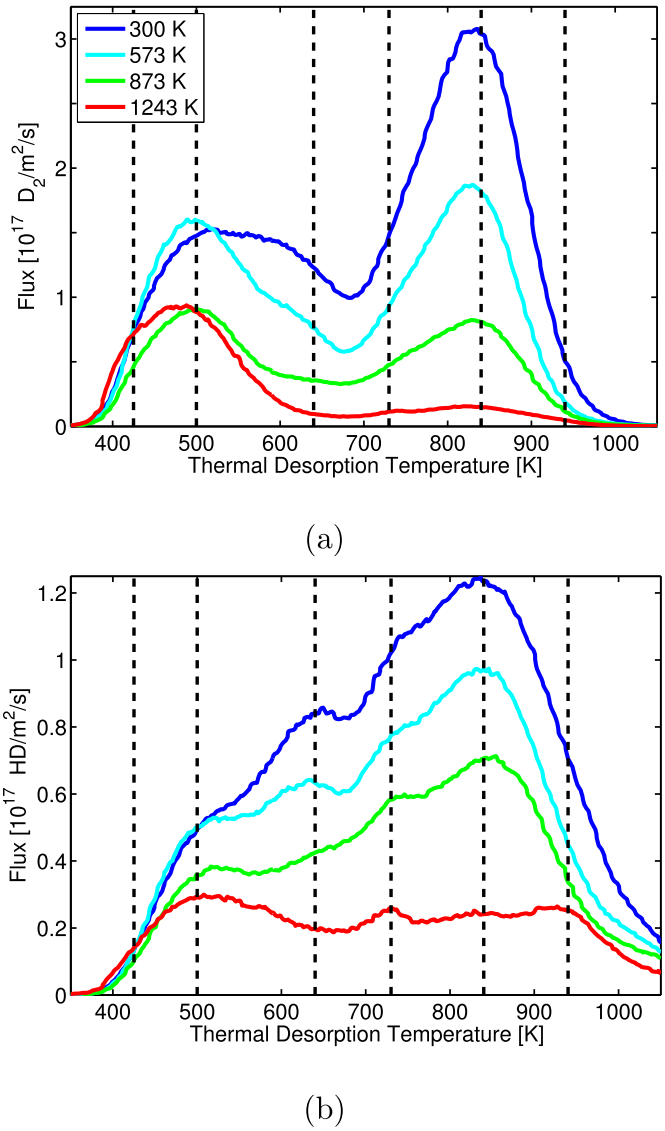

Fig. 3. The experimental TDS data for a) D2 and b) HD fluxes released from dynamically annealed damaged W. Samples damaged with Cu ions at RT (blue), 573 K (cyan), 873 K (green), and 1243 K (red) show reduced D retention. Release peaks identified by eye are marked near 425, 500, 640, 730, 840 and 940 K (vertical dashed black). (For interpretation of the references to colour in this figure legend, the reader is referred to the Web version of this article.)

3. Expanding TMAP7

To expand the capabilities of TMAP7 we developed a PTTP scheme that simplifies the system of equations. Note that the source code was not modified, instead only the input files were adjusted. This scheme works by redefining the traps to be modeled into two classes: a class of actively releasing traps and all remaining traps that are lumped into a single class within a pseudo trap. This class of pseudo traps can actively trap D in solution, but have high enough detrapping energies so that trapped D atoms are not appreciably released at the current sample temperature. All of the primary equations utilized in TMAP are further defined in the TMAP user manual [12]. In this section, we discuss the mathematical model in detail in order to clearly define the pseudo trap concept and explain the applicability of the model to experimental results.

TMAP models the migration of hydrogenic species as the temporal evolution of the solute concentration, $\mathbf{C_s}$. The first term on the right hand side is the one-dimensional Fickian diffusion equation, where $\mathbf{D}$ is the diffusion constant:

$$\frac{\partial \mathbf{C_s}}{\partial \mathbf{t}} = \frac{\mathbf{d}}{\mathbf{dx}}\left(\mathbf{D}\frac{\mathbf{dC_s}}{\mathbf{dx}}\right) + \mathbf{S_s} - \sum_{\mathbf{k}=1}^{\mathbf{m}} \frac{\partial \mathbf{C_k}}{\partial \mathbf{t}} \tag{1}$$

The source of solute, $\mathbf{S_s}$, models the implantation of atoms during plasma exposure. The last term accounts for the interaction of solute with m distinct traps, where $\mathbf{C_k}$ denotes the filled concentration for the $\mathbf{k^{th}}$ trap. The sum of all traps, $\mathbf{1}$ through $\mathbf{m}$, act as a sink or source when solute is lost to empty traps or released from filled traps respectively. This competition between the trapping rate, $\mathbf{R_k^t}$, and release rate, $\mathbf{R_k^r}$, determines the time dependence of all filled traps:

$$\sum_{\mathbf{k}=1}^{\mathbf{m}} \frac{\partial \mathbf{C_k}}{\partial \mathbf{t}} = \sum_{\mathbf{k}=1}^{\mathbf{m}} (\mathbf{R_k^t} - \mathbf{R_k^r}) \tag{2}$$

Between trap sites, the solute concentration diffuses at a rate determined by the diffusion constant renormalized by the lattice parameter, λ. The probability of finding an empty trap of type $\mathbf{k}$ is the difference between the total concentration of the $\mathbf{k^{th}}$ trap, $\mathbf{C_k^0}$, and the filled trap concentration, $\mathbf{C_k}$, normalized by the number density, $\mathbf{N_W}$. Therefore the total trapping rate, summed over all $\mathbf{m}$ traps, is due to the probability of the diffusing solute finding an empty trap:

$$\sum_{k=1}^{m} R_k^t = \frac{D}{\lambda^2} C_s \sum_{k=1}^{m} \frac{C_k^0 - C_k}{N_w} \tag{3}$$

Noting that the summation can easily be applied to a subset of the total number of traps, we can separate the total trapping rate:

$$\sum_{k=1}^{m} R_k^t = \sum_{k=1}^{n-1} R_k^t + \sum_{k=n}^{m} R_k^t = \sum_{k=1}^{n-1} R_k^t + R_p^t \tag{4}$$

Without any approximation, this allows us to expand the total trapping rate into the trapping rate due to individual traps spanning **1** to **n** − 1 and a pseudo trap accounting for all additional traps ranging from **n** to **m**, as shown in eq. (4). It is useful now at this point to assume, again without loss of generality, that the detrapping energies are ordered from lowest to highest, i.e. **k** = 1 denotes the lowest detrapping energy, **k** = 2 denotes the next lowest, and so forth, with **k** = **m** denoting the deepest (i.e. highest energy) trap. Here we define the pseudo trap concentration as the sum of concentrations across all traps spanning **n** to **m** for both the total and filled concentrations respectively:

$$C_p^0 \equiv \sum_{k=n}^{m} C_k^0 \,, \quad C_p \equiv \sum_{k=n}^{m} C_k \tag{5}$$

With these definitions for the pseudo trap concentration, the trapping rate due to the pseudo trap, R_p^t, is given by:

$$R_p^t \equiv \frac{D}{\lambda^2} C_s \sum_{k=n}^{m} \frac{C_k^0 - C_k}{N_w} = \frac{D}{\lambda^2} C_s \frac{C_p^0 - C_p}{N_w} \tag{6}$$

Again, we point out that these expressions are exact.

Next we turn our attention to the release of atoms from filled traps. The atoms held in a trap, C_k, have a probability to escape that is a thermally activated Arrhenius process, the release rate coefficient. The pre-exponential factor is the attempt frequency, ν_0, and the detrapping energy, E_k, is the barrier to activation. The total release rate is then given by the sum:

$$\sum_{k=1}^{m} R_k^r = \sum_{k=1}^{m} \nu_0 \exp\left(\frac{-E_k}{k_B T}\right) C_k \tag{7}$$

Utilizing the previously defined pseudo trap in eq. (5), we would like to separate the release rate the same way as was done for the trapping rate. However, here the summation cannot be pulled through since the likelihood of release from the k^{th} trap is dependent on the corresponding detrapping energy, E_k. As such, the first **n** − 1 terms are exact while the pseudo release rate, R_p^r, must be an approximation:

$$\sum_{k=1}^{m} R_k^r = \sum_{k=1}^{n-1} R_k^r + \sum_{k=n}^{m} R_k^r \approx \sum_{k=1}^{n-1} R_k^r + R_p^r \tag{8}$$

Based on the release rate shown in eq. (7), it is reasonable to conjecture that the release rate for the pseudo trap also follows an Arrhenius dependence on temperature, $\alpha(T)$, and the filled pseudo trap concentration:

$$\sum_{k=n}^{m} R_k^r \approx R_p^r = \alpha(T) C_p \tag{9}$$

To determine the form of the approximation, we consider the two limiting cases. First, the extreme where all traps spanning **n** to **m** are completely empty is automatically satisfied by eq. (9) because the concentrations vanish. The second extreme of a completely filled pseudo trap, where $C_k \Rightarrow C_k^0$ for **k** = **n** to **m**, yields the following:

$$\sum_{k=n}^{m} \nu_0 \exp\left(\frac{-E_k}{k_B T}\right) C_k^0 = \alpha(T) C_p^0 \tag{10}$$

Solving for $\alpha(T)$ and rewriting equation (9), the pseudo trap release rate can be defined in terms of the total trap concentrations and the Arrhenius behavior of each trap spanning **n** to **m**:

$$R_p^r \equiv \left[\sum_{k=n}^{m} \nu_0 \exp\left(\frac{-E_k}{k_B T}\right) \frac{C_k^0}{C_p^0}\right] C_p \tag{11}$$

Once again, C_p denotes the filled pseudo trap concentration, and C_p^0 denotes the total pseudo trap concentration. The result is an effective pseudo trap release rate that is given by the weighted average of the probability per unit time that a trapped particle escapes from the k^{th} trap multiplied by the relative concentration of the k^{th} trap.

With the assumed ordering of the trap energies, the error of the approximate release rate introduced by using this pseudo release rate is dominated by the lowest trap energy:

$$\Delta_{error} = \sum_{k=n}^{m} R_k^r - R_p^r \approx \nu_0 \exp\left(\frac{-E_n}{k_B T}\right) \left[C_n - \frac{C_n^0}{C_p^0} C_p\right] \tag{12}$$

The primary motivation for using the pseudo trap is to exploit the fact that, relative to the sample temperature, traps with deep detrapping energies (i.e. high temperature release peaks) are nearly indistinguishable in that the release probability is small for all such traps. For instance, one measure of a trap is its residence time, the average time an atom spends in a trap with energy E_k calculated as the inverse of the release rate coefficient. During the implantation phase, at a specific temperature, a pseudo trap can be chosen to span the detrapping energies with residence times approaching or exceeding the total implantation time. This condition ensures that any atom that falls into a pseudo trap stays trapped for the duration of implantation. A diffusion front progresses into the material filling low energy traps partially and fully filling the higher energy traps. The approximation becomes an exact solution when the pseudo trap is completely filled, as seen in eq. (12). Furthermore, the low pseudo release rate is accurate until the sample temperature is raised to the point where the pseudo trap begins to appreciably release during the thermal desorption phase. This is when the reallocation of a given trap from the pseudo trap population to the active trap population must occur.

4. Verification of the PTTP scheme: simulating 3 traps with 2 traps

To verify that the PTTP scheme used in TMAP7 can model multiple traps with one pseudo trap, we outline the simulation of a system of 3 traps with well separated detrapping energies using only 2 traps within the TMAP7 model (referred to in this discussion as the pseudo solution). We then compare the pseudo solution with an exact solution obtained by using TMAP7 with 3 traps applied to this same system. This numerical exercise demonstrates the concept and outlines the PTTP scheme. For brevity, we choose to use the experimental conditions and simulation inputs previously outlined in section 2. That is, we reuse the trap concentrations for the best fit with 3 traps to the release of D from a W sample subjected to Cu ion beam damage at RT.

During D implantation in Phase I, traps 2 and 3 have residence times that exceed the total implantation time as seen in Fig. 4, which shows the total implantation duration (green horizontal

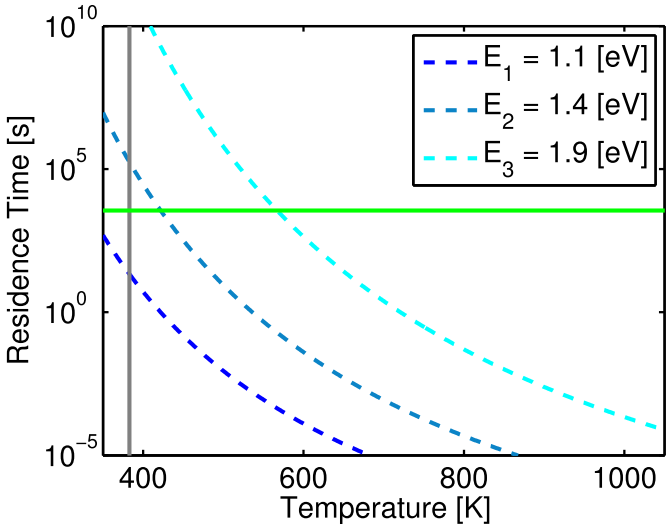

Fig. 4. The calculated residence times for traps 2 and 3 exceed total implantation time (horizontal light green) for the implantation temperature (vertical grey). (For interpretation of the references to colour in this figure legend, the reader is referred to the Web version of this article.)

line) for a sample held at 383 K (grey vertical line). Thus D atoms that are trapped in these two traps essentially stay there for the duration of the implantation. It thus stands to reason that the populations trapped within these two distinct traps can be viewed as a single population that is trapped for long periods of time. Incorporating this assumption into TMAP7, we simulate the diffusion and trapping of the implantation phase with trap 1 and a pseudo trap composed of traps 2 and 3, yielding the result shown in green in Fig. 5. Comparing this pseudo solution to the exact result also shown in Fig. 5 demonstrates that simplifying the set of equations with a single pseudo trap accurately reproduces the exact solution of the D depth profile with a residual error across the entire trapped D profile that is well below 1%.

Next, we apply the TMAP7 model to Phase II of the experiment, i.e. the controlled thermal desorption step. Below a temperature of 555 K there is little deviation between the surface flux of the exact and pseudo solutions as shown in Fig. 6. In this temperature regime only trap 1 is releasing while traps 2 and 3 are not appreciably releasing particles. We note that a transition occurs near a temperature where the pseudo trap begins to appreciably release, in this case a temperature near the trough between the first and second release peaks. We choose to define this as a transition temperature, that is the temperature where the exact and pseudo solutions begin to deviate significantly. As noted previously, the lowest energy trap within the pseudo trap dominates the error and produces the large secondary peak in Fig. 6.

Fig. 7 plots the total inventory of atoms held in each trap as a function of desorption temperature. The trap inventory is a better measure of release than the surface flux, since the latter is coupled to the diffusion and recombination processes. It can easily be seen that the pseudo trap begins to release at a transition temperature of 555 K (vertical dashed orange). Failure to account for the onset of this release process causes the pseudo-solution to then significantly deviate from the exact solution.

To recover the correct desorption profile, the model must be modified at this transition temperature to account for the onset of release from the higher energy traps. Examining Fig. 7, we note that at the transition temperature, trap 1 is nearly empty. Above the transition temperature, we can therefore safely neglect this lowest energy trap from the subsequent time evolution of the coupled equations, and in this simple example we can separate trap 2 out of the pseudo trap, leaving trap 3 explicitly within the pseudo trap. Solving the resulting two equations for the evolution of trap 2 and the remaining pseudo trap (which in this simple example only consists now of trap 3) then yields the PTTP scheme TDS profile shown in Fig. 8. Note that this approximate solution has only a minimal deviation from the exact solution obtained by tracking the evolution of all three traps simultaneously. This simple example therefore demonstrates that, as long as the lowest energy active trap can be considered to become depopulated before the next higher energy trap begins to release atoms, then this PTTP scheme can reduce the number of equations to be solved at any given temperature.

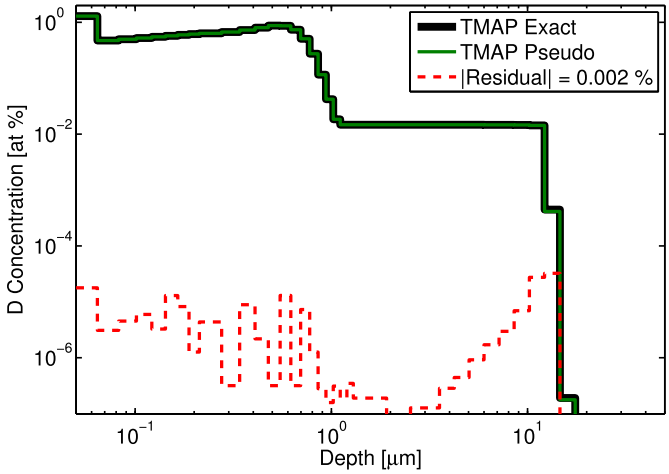

Fig. 5. The residual error (dashed red) between the exact (thick black) and pseudo (green) solutions for the D depth profile (i.e. after the implantation phase). Note that the exact solution is the sum of D filling traps 1–3, whereas the pseudo solution is the sum of trap 1 and the pseudo trap. (For interpretation of the references to colour in this figure legend, the reader is referred to the Web version of this article.)

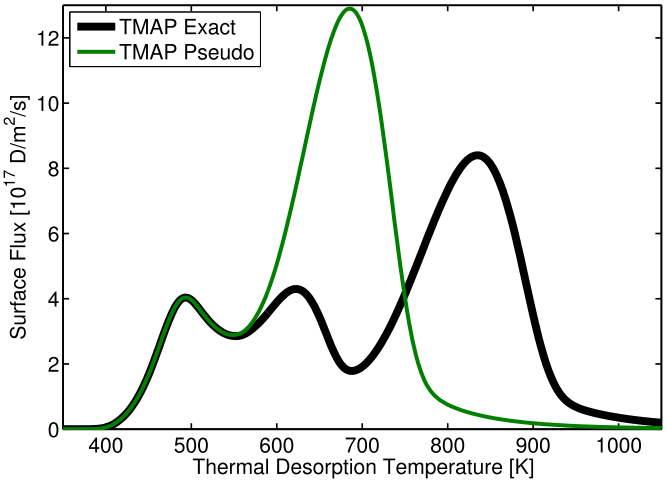

Fig. 6. The pseudo solution (green) with no temperature partition begins to deviate from the exact solution (thick black) as the temperature approaches the second release peak, which activates the lowest energy trap contained within the pseudo trap. (For interpretation of the references to colour in this figure legend, the reader is referred to the Web version of this article.)

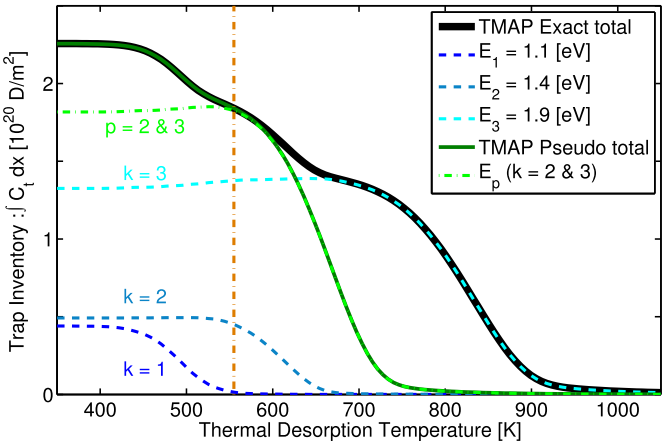

Fig. 7. The D inventory of each trap displays the trapping and release directly, without the effects of diffusion and surface recombination shown with the surface flux in Fig. 6. The total inventory for the exact solution (thick black) is the sum of traps 1–3, whereas the pseudo solution (dark green) is the sum of trap 1 (dashed blue) and the pseudo trap (dashed light green). The total for the exact and pseudo solutions deviate near the peak of the pseudo trap at 555 K (vertical dashed orange). (For interpretation of the references to colour in this figure legend, the reader is referred to the Web version of this article.)

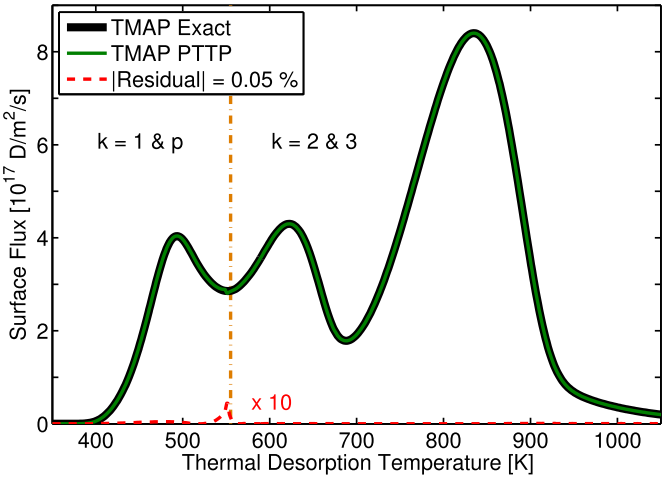

Fig. 8. PTTP scheme (green) applied using 2 traps at any given temperature. Below 555 K (vertical dashed orange), traps 1 and pseudo are modeled. Above 555 K, only traps 2 and 3 are modeled. The residual error (dashed red), magnified by 10, with respect to the exact solution (thick black) occurs primarily near the transition. (For interpretation of the references to colour in this figure legend, the reader is referred to the Web version of this article.)

5. Using the PTTP scheme to model D retention in damaged W with 6 traps

The results shown in Fig. 3 shows that the displacement-damaged W has six effective detrapping energies. This then suggests that we take the PTTP scheme further by incorporating additional traps to account for these six traps. Here we describe how the PTTP scheme can be used with TMAP7 to model the trapping and release of D from six distinct traps, and successfully reconstruct the implantation and thermal desorption of D in the RT damaged W sample described in Ref. [14].

As previously stated for the 3 trap TMAP simulation, the three spatial zones for traps have respective concentrations for each trap.

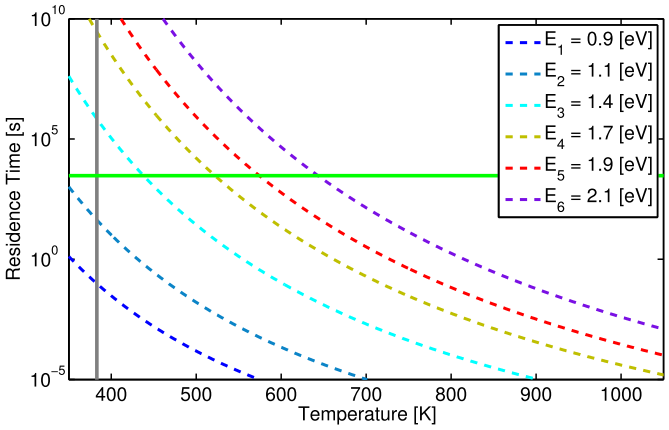

Fig. 9. The calculated residence time for traps 3–6 exceed the total implantation time (horizontal light green) for the implantation temperature (vertical grey). Thus traps 3–6 can be well modeled as one pseudo trap in the implantation phase. (For interpretation of the references to colour in this figure legend, the reader is referred to the Web version of this article.)

In this case, for six traps, the total number of adjustable concentrations is 18; we can simplify the modeling as follows. First it is reasonable to assume all 6 traps have a spatially uniform intrinsic background concentration. Second, from the undamaged W control sample, the near surface D concentration peak seen in the experimental NRA profile only shows a significant TDS release peak at low temperature. This observation then suggests that traps with the first three energies (0.9, 1.1, and 1.4 eV) are associated with near-surface plasma ion implantation induced defects. These are likely dislocations for the two lower and mono-vacancies for the last detrapping energy [6]. Similarly, comparing the TDS release peaks from undamaged and damaged samples suggests that only traps 3–6 are associated with energetic heavy ion induced damage. Therefore the number of free parameters is reduced from 18 to 13. Noting the previously quoted detrapping energies in similar experiments [2–7], the energy values are selected to correspond to the release peaks seen in the TDS data as shown in Fig. 3. We can then use these energies together with the known material properties to estimate the residence times for these traps. We find that during the D implantation phase, traps 3–6 fulfill the residence time requirement for the PTTP scheme as seen in Fig. 9 and thus we can lump these traps together into a single pseudo trap that will represent the net trapping effect due to all high energy traps. Note that all traps included in the pseudo trap have even longer residence time when held at RT. Only the lowest energy trap modeled, k = 1 may have appreciable release in the time between implantation and NRA.

Modeling active traps 1 and 2, together with this pseudo trap accounting for the higher energy traps (which do not release at the temperature of the implantation process) within TMAP7 then results in the modeled D profile arising from the implantation phase shown in Fig. 10. Comparing the result to the experimental NRA data in Fig. 10 shows reasonably good agreement, both in the first ~1 μm region where most of the trapped D resides and deeper into the material where D is trapped in the lower level of intrinsic traps.

Fig. 11 illustrates the total D held in each trap during the TDS release phase. Here the total inventory for trap k is simply the spatial integration of that traps filled concentration, $\mathbf{C_k}$, inferred from fitting the NRA profile as shown above together with the measured TDS release data. Initially the same trap scheme as used in the implantation is followed, with traps 1 and 2 modeled as active traps and the pseudo trap containing traps 3–6 (which at

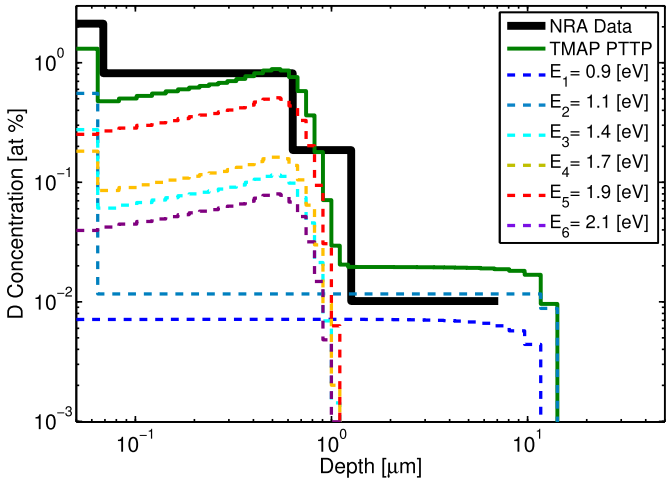

Fig. 10. The total D concentration simulated with PTTP (green) is the sum of all 6 trap concentrations (dashed lines) after the implantation phase. The pseudo trap is separated into its constituent traps 3 through 6. The NRMSE for the PTTP simulation is 0.7 with respect to the experimental NRA data (thick black), where 1 is a perfect fit. (For interpretation of the references to colour in this figure legend, the reader is referred to the Web version of this article.)

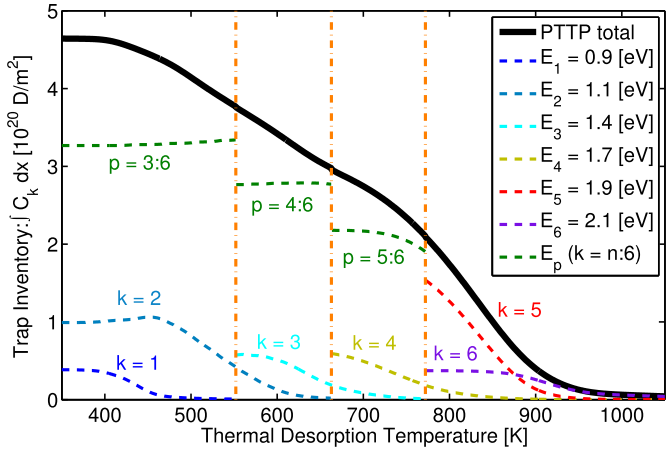

Fig. 11. The total D inventory in each trap as well as the total inventory (thick black). The discontinuity of the pseudo trap (dashed green) is due to removing the lowest energy trap in the pseudo trap at each transition temperature (vertical dashed orange). Also note that the lowest energy trap in each segment is neglected as it asymptotically approaches zero concentration at each transition temperature. (For interpretation of the references to colour in this figure legend, the reader is referred to the Web version of this article.)

low temperature do not release any D). As the temperature increases to 470 K, trap 1 is nearly empty, and the pseudo trap begins to significantly release D. At this transition temperature, trap 1 is removed from the simulation and the pseudo trap is adjusted to remove trap 3, which now becomes an active trap that releases (and traps) D atoms. The simulation continues into the next temperature segment with traps 2 and 3 as well as the adjusted pseudo trap, which now contains the summation of traps 4 through 6. The process continues with each additional temperature segment as shown in Fig. 11, each time removing the lowest remaining detrapping energy and adjusting the pseudo trap until eventually only traps 4, 5, and 6 remain in the final segment. The resulting desorption profile is compared to the experimental TDS data shown in Fig. 12. The results show that the residual error was significantly reduced from 25% to 4% utilizing 6 traps instead of 3.

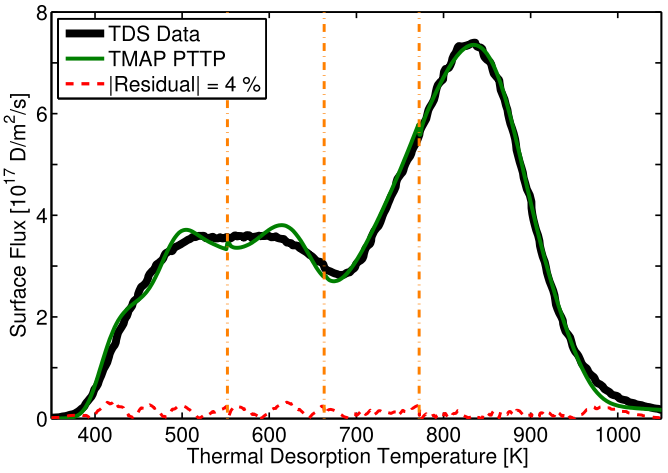

Fig. 12. The full PTTP simulation (green) with 6 traps compared to experimental RT damaged W (thick black). The residual error (dashed red) is 4% and the NRMSE is 0.95. (For interpretation of the references to colour in this figure legend, the reader is referred to the Web version of this article.)

6. Discussion

The applicability of this PTTP scheme is dependent on the overlap of release from traps with the lowest and the highest detrapping energies within a temperature segment. The error has two sources. First, neglecting the lowest detrapping energy by removing it from the set of coupled equations at the transition temperature cuts off the asymptotic tail of its release. Second, approximating the highest detrapping energy which is beginning to release within a temperature segment (i.e. the lowest detrapping energy within the pseudo trap) introduces the previously quantified error in eq. (12). The error increases when the tail of the release from the lowest energy trap overlaps significantly with the onset of release from the pseudo trap. That is, the detrapping energies and thus the release rate must be sufficiently separated. For instance, a separation of 0.05 eV while using 3 traps at a time would result in significant overlap of release during the TDS phase for the pseudo and lowest trap. Presented in Figs. 11 and 12, the $\sim$ 0.2 eV separation of detrapping energies ensured the lowest energy trap was nearly depopulated before the appreciable release of the pseudo trap. Unlike simply summing the release of uncoupled traps, this scheme retains the majority of the coupled trap interactions that occur.

The same methodology can be used to model multiple traps for other materials/solutes as well as adapted to other migration codes to improve the speed of simulations. It is well known that the additional coupled differential equations can significantly increase computation time. Both a high number of steps chosen in the discretized spatial grid or a large number of inactively releasing traps would be reasons to implement the method. That is, the computations saved using this method can be weighed against the additional computation needed to verify what temperature to transition and adjust the pseudo trap.

We note that there are other computational codes capable of solving systems involving more than three traps, but few of them have been recognized as verified and validated over as wide a range of experiments as TMAP. There are also several advantages to the use of TMAP7. A key feature of TMAP is the speed of simulations that can be run on a single processor. Lastly, we reiterate that the PTTP scheme does not fundamentally change the reaction-diffusion equations used in TMAP7. Instead, the scheme provides the framework to reduce the number of equations needed to model the trapping and release of solute atoms.

7. Summary

Utilizing TMAP7, we showed that three detrapping energies can not accurately represent the observed NRA and TDS profiles from our recent experiment [14]. By re-evaluating the HD flux of the TDS profiles, at least 6 distinct release peaks are observable. In order to simulate the experiment with only 3 traps at a given time, we developed a PTTP scheme to model multiple traps with a reduced number of equations. We further outlined the criteria by which to switch off inactive traps and track the most active traps. While this method introduces an error into the implantation and TDS phases, we show how to minimize the error through partitioning the temperature into segments. Lastly, the PTTP scheme was applied to simulate and experiment and shown to fit the data well.

Acknowledgments

This work was supported by U.S. Department of Energy under DE-FG02-07ER54912 and DE-SC0001999 as well as the University of California Office of Presidential Research Fund under 12-LR-237801.

References

[1] V. Philipps, Tungsten as material for plasma-facing components in fusion devices, J. Nucl. Mater. 415 (2011) S2–S9. Proceedings of the 19th International Conference on Plasma-Surface Interactions in Controlled Fusion.
[2] L. Buzi, G.D. Temmerman, D. Matveev, M. Reinhart, T. Schwarz-Selinger, M. Rasinski, B. Unterberg, C. Linsmeier, G.V. Oost, Surface modifications and deuterium retention in polycrystalline and single crystal tungsten as a function of particle flux and temperature, J. Nucl. Mater. 495 (2017) 211–219.
[3] A. Založnik, S. Markelj, T. Schwarz-Selinger, K. Schmid, Deuterium atom loading of self-damaged tungsten at different sample temperatures, J. Nucl. Mater. 496 (2017) 1–8.
[4] S.-Y. Qin, S. Jin, D.-R. Zou, L. Cheng, X.-L. Shu, Q. Hou, G.-H. Lu, The effect of inert gas pre-irradiation on the retention of deuterium in tungsten: a tmap investigation combined with first-principles method, Fusion Eng. Des. 121 (2017) 342–347.
[5] O. Ogorodnikova, J. Roth, M. Mayer, Deuterium retention in tungsten in dependence of the surface conditions, J. Nucl. Mater. 313–316 (2003) 469–477. Plasma-Surface Interactions in Controlled Fusion Devices 15.
[6] O.V. Ogorodnikova, J. Roth, M. Mayer, Ion-driven deuterium retention in tungsten, J. Appl. Phys. 103 (2008), 034902.
[7] M. Poon, A. Haasz, J. Davis, Modeling deuterium release during thermal desorption of d+ -irradiated tungsten, J. Nucl. Mater. 374 (2008) 390–402.
[8] Standard practice for neutron radiation damage simulation by charged-particle irradiation, e521-96, Annual Book of ASTM Standards 12.02, 1996, p. 8.
[9] R. Stoller, M. Toloczko, G. Was, A. Certain, S. Dwaraknath, F. Garner, On the use of {SRIM} for computing radiation damage exposure, Nucl. Instrum. Methods Phys. Res. Sect. B Beam Interact. Mater. Atoms 310 (2013) 75–80.
[10] J. Ziegler, J. Biersack, U. Littmark, The Stopping and Range of Ions in Matter, Pergamon Press, 1985.
[11] B. Merrill, J. Jones, D. Holland, Tmap/mod 1: Tritium Migration Analysis Program Code Description and User's Manual, Idaho National Engineering Laboratory EGG-ep-7407, EG and G, 1986.
[12] G. Longhurst, Tmap7 User Manual, Idaho National Engineering and Environment Laboratory INEEL/EXT-04-02352(Rev. 2), 2008.
[13] J. Ambrosek, G. Longhurst, Verification and Validation of Tmap7, Idaho National Engineering and Environment Laboratory INEEL/EXT-04–01657 (Rev. 2), 2008.
[14] M. Simmonds, Y. Wang, J. Barton, M. Baldwin, J. Yu, R. Doerner, G. Tynan, Reduced deuterium retention in simultaneously damaged and annealed tungsten, J. Nucl. Mater. 494 (2017) 67–71.
[15] W. Eckstein, Calculated Sputtering, Reflection and Range Values, IPP-report IPP 9/132, 2002.
[16] M. Baldwin, R. Doerner, Hydrogen isotope transport across tungsten surfaces exposed to a fusion relevant he ion fluence, Nucl. Fusion 57 (2017), 076031.
[17] D. Terentyev, A. Dubinko, A. Bakaeva, G.D. Temmerman, Strong sub-surface plastic deformation induced by high flux plasma in tungsten, Fusion Eng. Des. 124 (2017) (2016) 405–409. Proceedings of the 29th Symposium on Fusion Technology (SOFT-29) Prague, Czech Republic, September 5-9.